Evaluation of the Thermal Performance of Two Nonstandard Borehole Configurations

Parham Eslami-nejad, PhD

Michel Bernier, PhD, PE
Member ASHRAE

Odile Cauret, PhD

ABSTRACT

A theoretical study on the alternatives to single and double U-tube boreholes is presented in this work. These nonstandard configurations consist of channels arranged in a semicircle or in quadrants. Channels are thermally insulated to reduce the thermal short circuit between the downward and the upward legs.

The steady-state thermal performance of the proposed configurations is evaluated using an analytical solution for a set of coupled linear differential equations of energy balances with and without thermal interaction. The borehole thermal resistance and the circulating-fluid temperature during heat extraction are evaluated in the turbulent and laminar regimes and are used for comparison purposes. Results show that the new configurations offer up to a 20% reduction in borehole thermal resistance leading to shorter boreholes. For low mass flow rates (laminar flow), where thermal interaction between the upward and downward flowing fluid becomes more important, thermal insulation between channels can reduce the borehole thermal resistance of the proposed configurations by up to 15% over a standard double U-tube borehole configuration.

INTRODUCTION

Ground coupled heat pumps combined with vertical geothermal boreholes are noew widely proposed for space conditioning and hot-water production in net zero or highly efficient buildings. However, drilling costs associated with vertical boreholes remain a barrier for widespread utilisation particularly for small residential buildings.

Several studies have been conducted to improve the performance of vertical boreholes to reduce the required borehole length, and, thus the associated cost. These studies, which are reviewed in the following paragraphs, concentrated on the effect of using thermally enhanced materials for the grout and the pipes and improving borehole configurations.

Allan and Kavanaugh (1999) performed laboratory studies to measure the thermal conductivity of cementitious grouts containing different fillers. They also determine theoretically the influence of using such grouts on the borehole length. They concluded that depending on bore diameter and soil thermal conductivity, borehole length could be reduced by 22%–37% for a 100 ton (352 kW) load test case compared to cement-based grouts.

Remund (1999) performed laboratory studies to determine the effect of grout thermal conductivity, borehole diameter, pipe size, and pipe configuration on the total borehole thermal resistance. He reported that the borehole thermal resistance decreased by up to 19% with increasing grout thermal conductivity, which can, in turn, shorten the required borehole length. However, he found that increasing grout thermal conductivity over 1.7 W/m·K (1 Btu·h^{-1}·ft·°F^{-1}) provided very small additional reductions.

Acuna and Palm (2009) presented recommendations for improving the coefficient of performance of ground source heat pump (GSHP) systems by 10%–20% using better designed geothermal boreholes. They performed field testing of six borehole configurations under forced fluid circulation and two configurations under natural circulation. The annular coaxial configuration in forced circulation showed low temperature differences between the fluid and the borehole wall since the annular channel was in direct contact with the rock.

Raymond et al. (2011) performed two and three-dimensional numerical simulations to evaluate the performance of a newly developed high-density polyethylene (HDPE) pipes

Parham Eslami-nejad is a post-doctoral fellow at CanmetENERGY, Varennes, QC, Canada. **Michel Bernier** is a professor in the Département de génie mécanique, École Polytechnique de Montréal, Montréal, QC, Canada. **Odile Cauret** is a research engineer at Electricité de France, Moret-sur-Loing, France.

with a higher thermal conductivity. Results indicated that the thermally enhanced pipe reduces the borehole thermal resistance by up to 24% for single U-tube borehole, which reduces the required borehole length by up to 9% for specific loads conditions.

Platell (2006) proposed a so-called "TIL-pipe" configuration with one insulated pipe at the center for downward flow and several small pipes close to the borehole wall for upward flow. This configuration is used to reduce borehole thermal resistance as well as the pumping power. A 30% reduction in borehole thermal resistance is reported.

Luo et al. (2013) experimentally investigated the impact of borehole diameter on thermal performance. Eighteen boreholes in three different diameters were linked to a heat pump for air conditioning of an office building in Germany. A minor improvement of about 3.5% was reported between the largest diameter and the smallest one. However, they found that the smallest borehole diameter has the highest economic profitability.

Focaccia and Tinti (2013) proposed two new borehole configurations, one with a coaxial pipe and the other with a U-pipe. Both pipes are immersed in a water-antifreeze mixture surrounded by a protection system, as well as relatively thin ring of grout. The existence of natural convection in the water-antifreeze mixture was experimentally verified and a slight reduction of about 4% in the borehole thermal resistance was reported.

Eslami-nejad and Bernier (2011a, 2011b) proposed a new double U-tube borehole configuration with two independent circuits. With this configuration they were able to examine simultaneous heat injection and extraction in the borehole. They found that, for typical borehole characteristics, this configuration connected to a relatively low temperature heat source is shallower than single U-tube and regular double U-tube borehole configurations. The same authors used the new borehole configuration for solar heat injection during a heat extraction period in a cold climate condition (Eslami-nejad and Bernier 2012). The borehole was equipped with a ring of saturated sand to take advantage of the latent heat of water under freezing/thawing conditions. Based on several numerical annual simulations, they concluded that a reduction of up to 38% in borehole length is possible in low thermal conductivity grounds. In another study, they evaluated the effect of using phase change materials in the immediate vicinity of single U-tube borehole configurations in cooling dominated climate (Eslami-nejad and Bernier 2013). They performed several simulations over a cooling season and they reported a 9% reduction of the borehole length.

In summary, these studies show that it is possible to improve borehole thermal performance by using various techniques. The objective of this work is to investigate the thermal performance of two nonstandard borehole configurations. These two configurations are proposed to maximize the thermal contact with the ground and to minimize thermal interaction between the upward and downward flowing fluid. As shown in Figure 1, they consist of noncircular channels which are thermally insulated at the common boundaries and surrounded by a relatively thin ring of grout. The use of such configurations could lead to the reduction of the borehole diameter and to less expensive drilling techniques. Being an exploratory study, no attempt was made to have these pipe channels manufactured.

The configuration in Figure 1a is referred to here as the semicircle and Figure 1b as the quadrant. The steady-state thermal performance of these configurations is compared against commonly used double U-tube borehole.

MODEL DEVELOPMENT

In this section, steady-state heat transfer between the fluid and the borehole wall is modeled for the proposed borehole configurations. Temperature distribution over borehole depth, fluid outlet temperature, overall borehole thermal resistance, and heat transfer rate per unit length of the borehole are calculated. The analytical solution of the model is based on a few assumptions: it is assumed that the grout is homogeneous and its thermal properties are constant, the borehole wall temperature is constant along the borehole's depth as well as over the borehole perimeter, and heat conduction in the axial direction is negligible.

Borehole Configurations

a. Semicircle

This configuration consists of two half-circle channels connected back-to-back and separated using a thin layer of insulation as shown in Figure 1a. The channels are surrounded by a thin ring of grout. As shown in Figure 2a, the circulating fluid goes down in either the left or right channel and up in the other one.

Semicircle with thermal interaction. In this section, thermal interaction between channels through the insulation is taken into account. Therefore, the difference between the

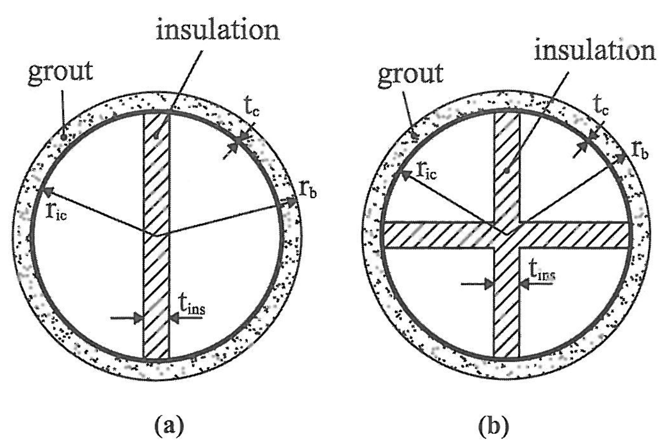

Figure 1 *Borehole cross sections: (a) semicircle and (b) quadrant boreholes.*

borehole wall temperature (T_b) and the fluid temperatures (T_{f1} and T_{f2}) in each channel is caused by the net heat flows per unit length in and out of the two channels. The vertical temperature distribution of the fluid is obtained by solving a set of coupled linear differential equations in which the horizontal heat transfer in the borehole cross section is obtained through conductive and convective resistances.

$$
\begin{aligned}
-\dot{m}c_p\frac{dT_{f1}(z)}{dz} &= \frac{T_{f1}(z)-T_b}{R'_1}+\frac{T_{f1}(z)-T_{f2}}{R'_{12}} \\
+\dot{m}c_p\frac{dT_{f2}(z)}{dz} &= \frac{T_{f2}(z)-T_{f1}}{R'_{21}}+\frac{T_{f2}(z)-T_b}{R'_2}
\end{aligned}
\tag{1}
$$

The z-coordinate direction is defined as downward (from the ground surface), and as indicated in Figure 2b, an outward heat flow is considered positive. Therefore, fluid in channel 1 flows in the downward direction.

Since the channels are positioned symmetrically in the borehole cross section, it is assumed that $R'_{12} = R'_{21}$ and $R'_1 = R'_2$. It is further assumed that the insulation thickness is very small compared to borehole diameter.

$$
\begin{aligned}
R'_1 = R'_2 &= \frac{1}{(\pi-2\alpha)r_{ic}h_c} \\
&+\frac{\ln[(r_{ic}+t_c)/r_{ic}]}{(\pi-2\alpha)k_c}+\frac{\ln[r_b/(r_{ic}+t_c)]}{\pi k_g}
\end{aligned}
\tag{2}
$$

$$
R'_{12} = R'_{21} = \frac{t_{ins}}{2yk_{ins}}+\frac{2}{(\pi-2\alpha)r_{ic}h_c} \tag{3}
$$

The first term on the right hand side of Equation 2 represents the convective thermal resistance of the fluid, while the second and the third terms are the conductive thermal resistances associated with the channel wall and the grout thicknesses, respectively. The values of h_c, k_c, and k_g are the convective heat transfer coefficient of the fluid flowing inside channels, and the thermal conductivities of the channel thickness and grout respectively. The value of y in Equation 3 and the angle α are defined later in this section (see Figure 2c).

Convection heat transfer coefficient (h_c) correlations for this geometry (and the quadrant) could not be found in the literature, and assumptions had to be made. First, considering the length of the borehole, it is assumed that the flow is fully developed. For the case of turbulent flow, it is assumed that correlations for circular cross sections can be used even though convection coefficients vary around the periphery, approaching zero in the corners, in a noncircular channel. The Nusselt number (Nu) is calculated using the Gnielinski correlation. In laminar flow, a uniform surface temperature is assumed with a corresponding Nusselt number of 3.66 (Kays and Crawford 1980). The hydraulic diameter of the channel is used for the calculation of the Reynolds number (Re). The hydraulic diameter is defined as four times the flow cross-sectional area divided by the wetted perimeter ($D = 4A_c/P$). The various geometric parameters are shown in Figure 2c.

$$
\begin{aligned}
\cos\beta &= t_{ins}/2r_{ic} \rightarrow \alpha = 90-\beta \\
y &= r_{ic}\sin\beta
\end{aligned}
\tag{4}
$$

$$
\begin{aligned}
l_2 &= 2\pi r_{ic}\frac{180-2\alpha}{360} \\
P &= l_2+2y
\end{aligned}
\tag{5}
$$

$$
A_c = \pi r_{ic}^2\frac{180-2\alpha}{360}-yt_{ins}/2
$$

$$
D_h = \frac{4\pi r_{ic}^2\frac{180-2\alpha}{360}-2yt_{ins}}{2\pi r_{ic}\frac{180-2\alpha}{360}+2y} \tag{6}
$$

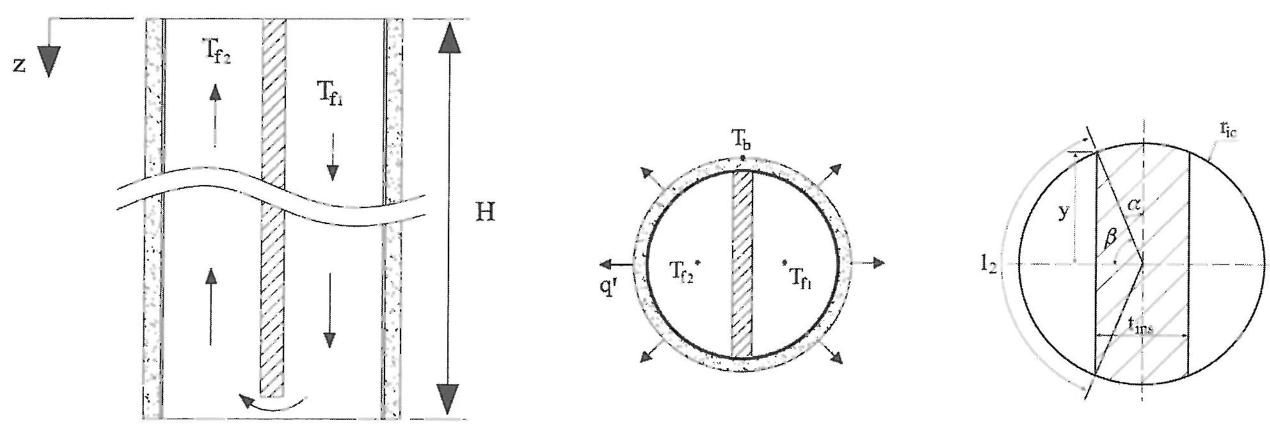

Figure 2 *Schematic representation of semicircle borehole configuration.*
**(Size of the dividing wall has been exaggerated for illustrative purposes.)*

Equation 1 is nondimensionalised, using the dimensionless variables listed in Equations 7 and 8.

$$\theta_1 = \frac{T_{f1}(z) - T_b}{T_{in} - T_b},\ \theta_2 = \frac{T_{f2}(z) - T_b}{T_{in} - T_b},\ Z = \frac{z}{H}$$
$$R_1^* = \frac{\dot{m}c_p R'_1}{H},\ R_{12}^* = \frac{\dot{m}c_p R'_{12}}{H} \tag{7}$$

$$-\frac{d\theta_1}{dZ} = (a+b)\theta_1 - b\theta_2$$
$$+\frac{d\theta_2}{dZ} = -b\theta_1 + (a+b)\theta_1 \tag{8}$$

where $a = \frac{1}{R_1^*},\ b = \frac{1}{R_{12}^*}$

Equation 8 is solved using Laplace transforms technique and the dimensionless temperature distributions, $\theta_1(Z)$ and $\theta_2(Z)$ are as follows:

$$\theta_1(Z) = G_{11}\exp(-\eta Z) + G_{12}\exp(\eta Z)$$
$$\theta_2(Z) = G_{21}\exp(-\eta Z) + G_{22}\exp(\eta Z) \tag{9}$$

The distribution functions $G_{11}(Z)$, $G_{12}(Z)$, $G_{21}(Z)$, and $G_{22}(Z)$ are

$$G_{11} = \frac{a+b-\theta''b-\gamma}{2\eta},\ G_{12} = \frac{\eta-a-b+\theta''b}{2\eta}$$
$$G_{21} = \frac{b-\theta''b-\theta''a-\theta''\gamma}{2\eta},\ G_{22} = \frac{\eta\theta''-b+\theta''b+\theta''a}{2\eta} \tag{10}$$

where

$$\eta = \sqrt{a(a+2b)} \tag{11}$$

$\theta'' = (T_{out} - T_b)/(T_{in} - T_b)$ is dimensionless outlet temperature and it is calculated by applying a boundary condition at the bottom of the borehole where $\theta_1(1) = \theta_2(1)$.

Using the outlet temperature and the net heat transfer to the ground per unit length of the borehole, q', the overall borehole thermal resistance, R'_{eff}, is calculated as follows:

$$R'_{eff} = \frac{T_f - T_b}{q'} \tag{12}$$

where $T_f = (T_{in} + T_{out})/2$.

Semicircle with no thermal interaction: In this section, it is assumed that the dividing wall between the channels is perfectly insulated and therefore there is no heat exchange between them. The governing equations are then

$$q' = \frac{T_f(z) - T_b}{R'_b} \tag{13}$$

$$q' = -2\dot{m}c_p\frac{dT_f(z)}{dz},\ T_f = T_{in} \text{ at } z = 0 \tag{14}$$

Since thermal interaction is neglected, the geometry is similar to a single channel with a depth $2H$ that exchanges heat only with the ground. Therefore, the axial fluid temperature variation is:

$$T_f(z) = T_b + (T_{in} - T_b) \times \exp\left(\frac{-z}{2R'_b\dot{m}c_p}\right) \quad 0 \le z \le 2H \tag{15}$$

where

$$T_f(z) = T_{f1}(z) \text{ for } z = 0 \text{ to } z = H$$

$$T_f(z) = T_{f2}(z) \text{ for } z = H \text{ to } z = 2H$$

R'_b is the borehole thermal resistance and it is calculated as

$$\frac{1}{R'_b} = \frac{1}{R'_1} + \frac{1}{R'_2} \tag{16}$$

where $R'_1 = R'_2$ and therefore $R'_b = R'_1/2$. R'_1 is calculated using Equation 2.

b. Quadrant

In this configuration, four identical quadrants are separated using thin insulated walls to minimize thermal interaction between them (see Figure 3b). These four pieces are surrounded by a thin ring of grout. For this configuration, flow circulation can be categorized either as being in series or in parallel.

In the series arrangement, as shown in Figure 4a, the circulating fluid goes down into one of the channels first and then it flows through the others, one by one.

In the parallel arrangement, Figure 4b, the flow rate is divided in two equal streams and each stream goes down one channel and up from the other. If thermal interaction between channels is taken into account, different combinations of circuit arrangements can be considered.

In this study, thermal interaction is taken into account only for the parallel configuration as the effect on the series configuration is not significant. The 1-3, 2-4 arrangement is used for the parallel configuration. The fluid in the first circuit enters channel #1 goes to the bottom of the borehole and then up channel #3 and the fluid in the second circuit enters channel #2 goes to the bottom of the borehole and then up channel #4.

1-3, 2-4 parallel arrangement with thermal interaction: For this circuit configuration $T_{f1}(z) = T_{f2}(z)$ and

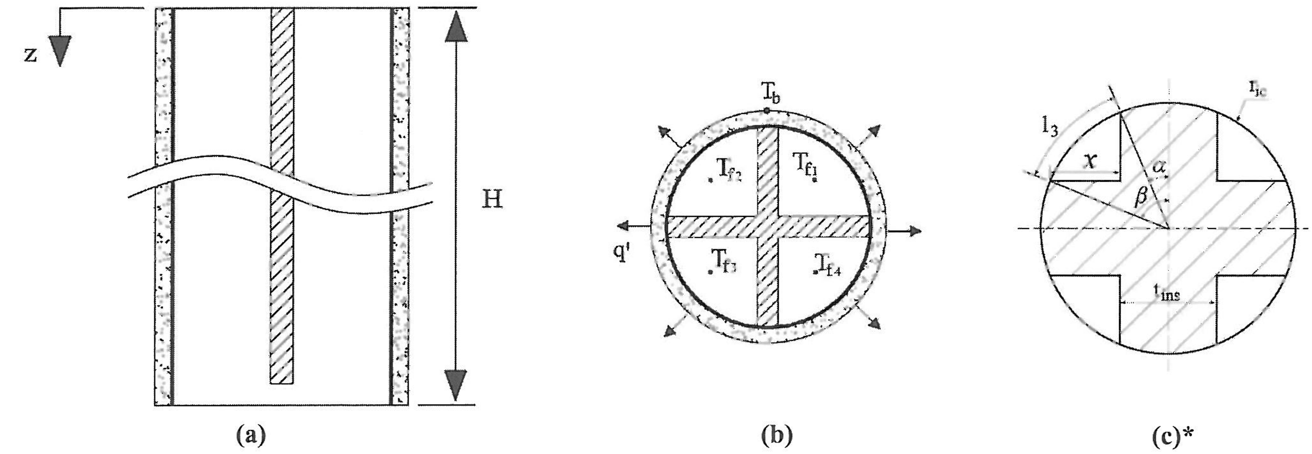

Figure 3 *Schematic representation of the quadrant configuration.*
**(Size of the dividing wall has been exaggerated for illustrative purposes.)*

$T_{f3}(z) = T_{f4}(z)$ due to symmetry. Therefore, the energy conservation equation can be written as follows:

$$-\dot{m}c_p\frac{dT_{f1}(z)}{dz} = \frac{T_{f1}-T_b}{R'_1} + \frac{T_{f1}-T_{f3}}{\frac{R'_{12}R'_{13}}{R'_{12}+R'_{13}}}$$
$$+\dot{m}c_p\frac{dT_{f3}(z)}{dz} = \frac{T_{f3}-T_{f1}}{\frac{R'_{12}R'_{13}}{R'_{12}+R'_{13}}} + \frac{T_{f3}-T_b}{R'_1} \tag{17}$$

Thermal interaction between channels 1 and 3 is negligible due to insignificant shared boundaries. Therefore, Equation 17 turns out to be identical to Equation 1; however, R'_1 and R'_{12} have to be replaced with the following equations:

$$R'_1 = \frac{1}{(\pi/2-2\alpha)r_{ic}h_c} + \frac{\ln[(r_{ic}+t_c)/r_{ic}]}{(\pi/2-2\alpha)k_c} + \frac{\ln[r_b/(r_{ic}+t_c)]}{\pi k_g/2} \tag{18}$$

$$R'_{12} = \frac{t_{ins}}{xk_{ins}} + \frac{2}{(\pi/2-2\alpha)r_{ic}h_c} \tag{19}$$

The first term on the right hand side of Equation 18 represents the convective thermal resistance of the fluid while the second and the third terms are conductive thermal resistances associated with the channel wall and the grout thicknesses, respectively. The parameters h_c, k_c, and k_g have been defined earlier for the semicircle configuration while other terms are presented in Figure 1b. Angle α and parameter x are calculated below (see Figure 3c).

The same correlations as the ones used for the semicircle configuration are used to calculate the convection heat transfer coefficient (h_c) in the laminar and turbulent regime. However, the hydraulic diameter (D_h) of the channel is calculated as follows:

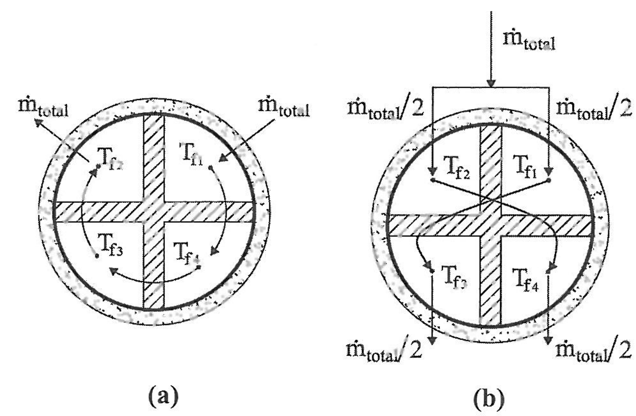

Figure 4 *Schematic representation of (a) series and (b) parallel arrangements.*

$$\cos\beta = (t_{ins}/2r_{ic}) \rightarrow \alpha = 90-\beta$$
$$x = r_{ic} - \sin\beta - t_{ins}/2 \tag{20}$$

$$l_3 = 2\pi r_{ic}\frac{\beta-a}{360}$$
$$P = l_3 + 2x$$
$$A_c = \pi r_{ic}^2\frac{\beta-a}{360} - \frac{r_{ic}t_{ins}/2}{\sin\frac{\beta+\alpha}{2}}\sin\frac{\beta-\alpha}{2} \tag{21}$$

$$D_h = \frac{4\pi r_{ic}^2\frac{\beta-\alpha}{360} - \frac{2r_{ic}t_{ins}}{\sin\frac{\beta+\alpha}{2}}\sin\frac{\beta-\alpha}{2}}{2\pi r_{ic}\frac{\beta-\alpha}{360} + 2x} \tag{22}$$

It has to be noted that the dimensionless thermal resistances are calculated based on the mass flow rate in each circuit ($\dot{m}_{total}/2$). Equation 9 can be also used here for the dimensionless temperature distribution of the parallel arrangement with thermal interaction. Equation 13 is used to calculate the overall borehole thermal resistance in which q' is the total heat transfer to the ground per unit length of the borehole.

Parallel arrangement without thermal interaction: If perfect insulation is assumed in the separating walls, heat transfer between channels is ignored and the channel sequence does not matter anymore. Therefore, two identical circuits are considered with the heat balance equation as follows:

$$\frac{q'}{2} = \frac{T_f(z) - T_b}{R'_b} \tag{23}$$

where

$$q' = -4 \times \frac{\dot{m}_{total}}{2} c_p \frac{dT_f(z)}{dz}, \; T_f = T_{in} \text{ at } z = 0 \tag{24}$$

T_{fU} is the upward fluid temperature and T_{fD} is the downward fluid temperature. Fluid temperature distribution for each circuit is written as

$$T_f(z) = T_b + (T_{in} - T_b) \times \exp\left(\frac{-z}{R'_b \dot{m}_{total} c_p}\right) \quad 0 \le z \le 2H \tag{25}$$

Equation 25 is used for the downward fluid within the range of $z = 0$ to $z = H$ and it is used for the upward fluid within the range of $z = H$ to $z = 2H$. R'_b is the borehole thermal resistance, evaluated using Equation 13, and due to symmetry it is equal to R'_1, which is obtained by dividing Equation 18 by two.

Series arrangement without thermal interaction. Channel sequence is not important. The heat balance equation can be written as

$$q' = \frac{T_f(z) - T_b}{R'_b} \tag{26}$$

where

$$q' = -4 \times \dot{m}_{total} c_p \frac{dT_f(z)}{dz}, \; T_f = T_{in} \text{ at } z = 0 \tag{27}$$

T_{f1}, T_{f2}, T_{f3} and T_{f4} are the fluid temperatures along the first, second, third and the forth channels, respectively. Since there is no thermal interaction between channels, it is assumed that a $4H$ long channel exchanges heat only with the ground. Therefore, the fluid temperature distribution can be written in the following form:

$$T_f(z) = T_b + (T_{in} - T_b) \times \exp\left(\frac{-z}{4R'_b \dot{m}_{total} c_p}\right) \quad 0 \le z \le 4H \tag{28}$$

where

$$T_f(z) = T_{f1}(z) \text{ for } z = 0 \text{ to } z = H$$

$$T_f(z) = T_{f2}(z) \text{ for } z = H \text{ to } z = 2H$$

$$T_f(z) = T_{f3}(z) \text{ for } z = 2H \text{ to } z = 3H$$

$$T_f(z) = T_{f4}(z) \text{ for } z = 3H \text{ to } z = 4H$$

R'_b is equal to $R'_1/4$ where R'_1 is evaluated using Equation 18.

RESULTS

Fluid temperature profiles and borehole thermal resistances of the two new configurations are compared against those of a typical double U-tube configuration. In order to have a fair comparison, borehole depth, flow regime, borehole diameter, minimum distance between pipe wall and borehole wall and fluid mass flow rate are set equal for all three configurations. Borehole characteristics are listed in Table 1. Results are arranged as follows. First, a base case is presented where thermal interaction through the insulating wall is accounted for. The impact of thermal interaction is then examined for the semicircle configuration. This is followed by the the analysis of the effect of an increase/decrease of the grout thermal conductivity. Borehole dimensions are then varied to examine their effect on borehole thermal resistance. Finally, the effects of a low flow rate condition are quantified.

The double U-tube borehole configuration is presented schematically in Figure 5. According to the dimensions listed in Table 1, pipes are positioned midway between the borehole center and the borehole wall (typically referred to as the B configuration). The 1-3, 2-4 parallel arrangement is used for the double U-tube configuration since it offers the lowest borehole thermal resistance among all other arrangements (Zeng et al. 2003). The fluid temperature distribution function and borehole thermal resistance given by Zeng et al. (2003) are used here for calculations related to this configuration.

The inlet fluid temperature and borehole wall temperature for all three configurations are set to 0°C (32°F) and 10°C (50°F), respectively. With the fluid mass flow rate given in Table 1 the flow regime is turbulent in all configurations (i.e., Re > 2300) for this set of results.

a. Base case

Figure 6 presents the fluid temperature evolution over borehole depth for the three configurations. Thermal interaction through the insulating walls is taken into account for the semicircle and parallel quadrant configurations. The series quadrant (denoted as S.Q. in Figure 6) is also shown. As shown in Figure 6, all configurations perform equally over the first

Table 1. Borehole Characteristics of the Semicircle, Quadrant and Double U-Tube Configurations

	Units	Semicircle	Quadrant	Double U-tube
$\dot{m}$	kg/s (lb/s)	0.3 (0.66)		0.3 (0.66)
r_b		7 (2.75)		7 (2.75)
r_{ic}		3.95 (1.55)		—
t_c		0.25 (0.098)		—
t_{ins}	cm (in.)	0.5 (0.197)		—
r_{it}		—	—	1.1 (0.43)
t_t		—	—	0.25 (0.098)
2D		—	—	5.7 (2.24)
k_g		2 (1.16)		2 (1.16)
k_c	$W \cdot m^{-1} \cdot K^{-1}$ ($Btu \cdot h^{-1} \cdot ft^{-1} \cdot {}^{\circ}F^{-1}$)	0.4 (0.23)		—
k_p		—	—	0.4 (0.23)
k_{ins}		0.05 (0.029)		—
H	m (ft)	100 (328)		100 (328)

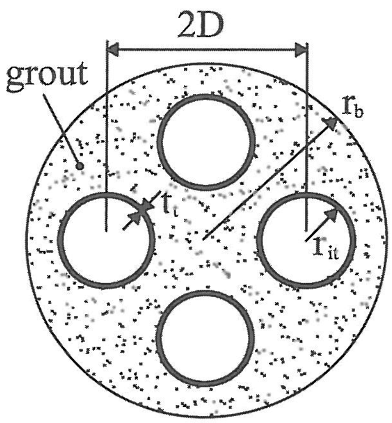

Figure 5 Schematic representation of the double U-tube configuration.

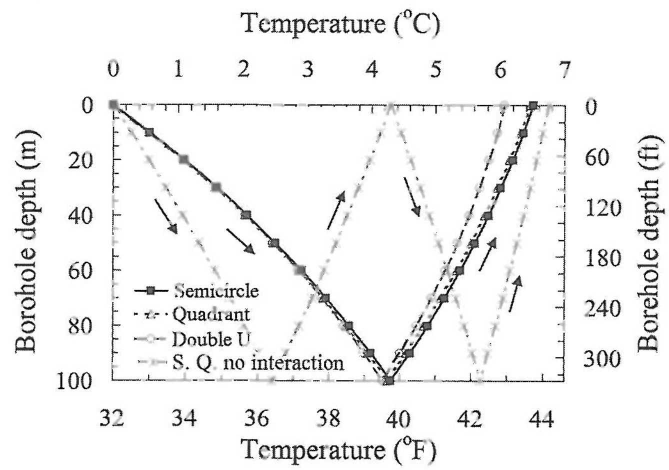

Figure 6 Fluid temperature profile of semicircle, series and parallel quadrant and double U-tube configurations.

leg with only slight differences. However, the fluid temperature inside the double U-tube starts deviating from the other two in the upward leg. This is due to the fact that the channels in the semicircle and quadrant configurations interact thermally more with the ground and less between each other compared to the double U-tube configuration. The outlet fluid temperature of the semicircle configuration is the highest (6.51°C [43.7°F]) followed very closely by the quadrant geometry (6.46°C [43.6°F]) and then by the double U-tube configuration at 6.06°C (42.9°F). As shown in Table 2, the borehole thermal resistance of the semicircle configuration is equal to 0.082 $K \cdot m \cdot W^{-1}$ (0.143 $ft \cdot {}^{\circ}F \cdot Btu^{-1} \cdot h$). The corresponding value for the double U-tube is 11% higher. The best configuration would be the series quadrant configuration without thermal interaction with an outlet temperature of 6.78°C (44.2°F) and with a 16% reduction in the borehole thermal resistance compared to the double U-tube configuration.

b. Effect of thermal interaction for the semicircle configuration

As shown in Figure 7, the effect of thermal interaction between channels on the fluid temperature profile is insignificant

Table 2. Borehole Thermal Resistance Calculated for Different Cases

			Borehole Thermal Resistance					
			Semicircle + Interaction	Semicircle No Interaction	P.Q. + Interaction	P.Q. No Interaction	S.Q. No Interaction	Double U-tube
Base case		(K·m·W^{-1})*	0.0824	0.0808	0.0833	0.0818	0.0782	0.0914
Change	k_g high		0.0704	0.0688	0.071	0.0697	0.0662	0.0740
	k_g low		0.1207	0.1191	0.1216	0.1201	0.1162	0.1467
	r_b		0.0529	0.0514	0.0536	0.0522	0.0494	0.0561
	r_{ic}, r_{it}		0.0824	0.0806	0.0837	0.0820	0.0776	0.0875
	$\dot{m}$		0.4903	0.4036	0.4717	0.4003	0.4003	0.4616

* Multiply by 1.744 to get (ft°FBtu^{-1}h).

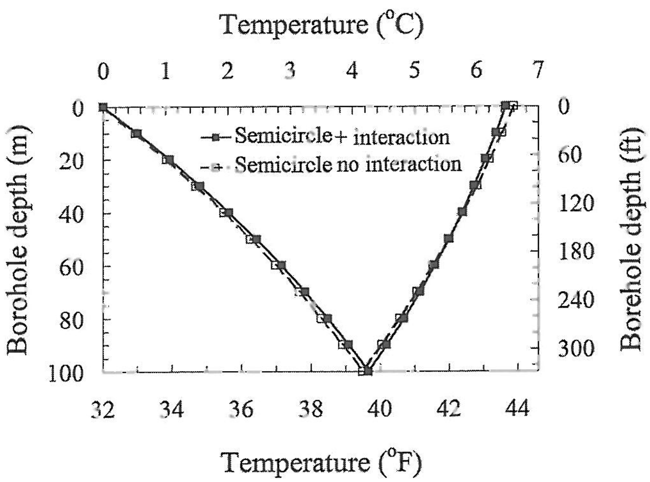

Figure 7 *Fluid temperature profile of semicircle configuration with and without thermal interaction between channels.*

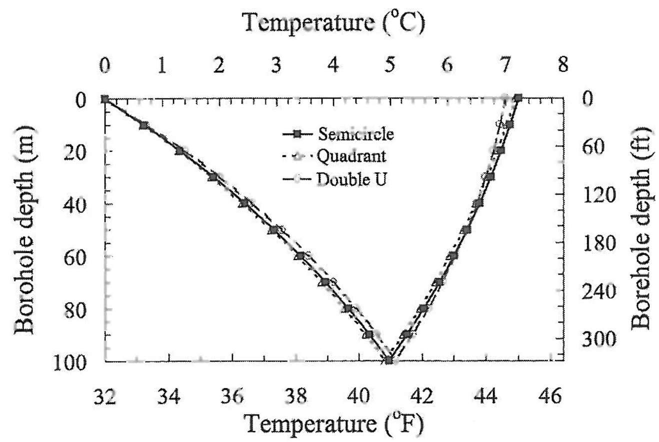

Figure 8 *Fluid temperature profile of the semicircle, quadrant and double U-tube configurations using thermally enhanced grout.*

for the semicircle configuration. Without thermal interaction between channels, the fluid outlet temperature increases by 0.2°C (32.4°F) and the borehole thermal resistance decreases by only 2%.

c. Effect of a change in the grout thermal conductivity

As shown in Figure 8, if the thermal conductivity of the grout is increased to 3 W·m^{-1}·K^{-1} (1.725 Btu·h^{-1}·ft^{-1}·°F^{-1}), the difference between the outlet fluid temperatures in the semicircle and double U-tube configurations turns out to be relatively small (0.23°C [0.41°F]). Furthermore, the fluid temperature profile for the double U-tube configuration approaches the ones for the semicircle and quadrant configurations. It is worth observing that the double U-tube configuration performs better over the first leg. However, due to the thermal short circuit between pipes it is less efficient as the borehole thermal resistance of the semicircle is 5% lower than that of the double U-tube configuration.

Conversely, if the thermal conductivity of the grout decreases to 1 W·m^{-1}·K^{-1} (0.575 Btu·h^{-1}·ft^{-1}·°F^{-1}), the difference between the semicircle and double U-tube configuration is more pronounced (see Figure 9). The semicircle is still the best configuration surpassing the quadrant by a 1% difference in borehole thermal resistance but with a 21% difference with the double U-tube configuration.

d. Effects of a change in borehole dimensions

In order to see the effect of having pipes and channels very close to the borehole wall, the borehole radius is reduced to 4.5 cm (1.75 in.) and all other dimensions are kept the same as presented in Table 1. As shown in Figure 10, the semicircle configuration is again superior to the quadrant and double U-tube configurations. The borehole thermal resistance of the semicircle configuration is 6% lower than the one for the

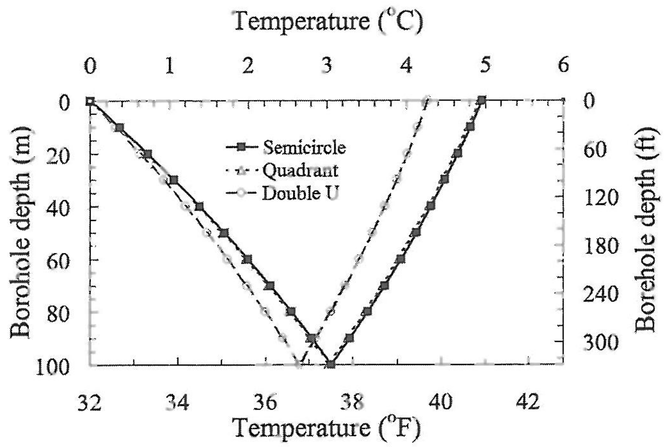

Figure 9 *Fluid temperature profile of the semicircle, quadrant and double U-tube configurations using a low thermal conductivity grout.*

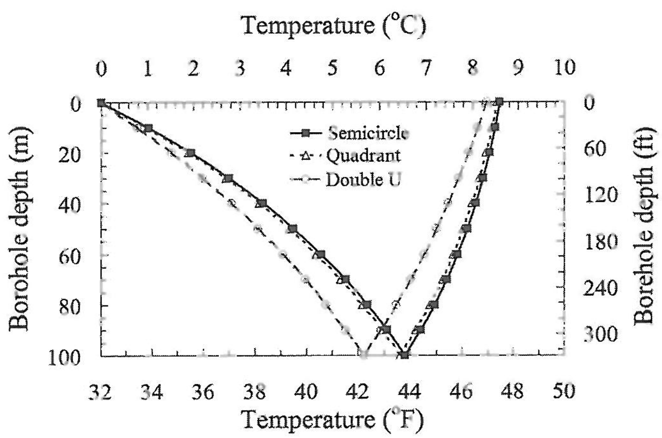

Figure 10 *Fluid temperature profile of semicircle, quadrant and double U-tube configurations for a reduced borehole radius.*

double U-tube configuration. There is a very small difference (1%) between the borehole thermal resistance of the semicircle and quadrant configurations. However, contrary to what is shown in Figures 8 and 9, the double U-tube configuration performs better over the second leg while the semicircle and quadrant configurations are better along the first leg.

The following changes are made to the borehole characteristics listed in Table 1 to evaluate the effect of pipe and channel sizes. For the double U-tube configuration, the nominal size of the pipe diameter is increased from 19 to 37 mm (¾ to 1½ in.). In order to keep the same clearance between channels and the borehole wall in the semicircle configuration and between pipes and borehole wall in double U-tube configuration, channel radius is also increased accordingly (see Table 3). For this case, the borehole thermal resistance of the semicircle is 6% lower than double U-tube configuration.

Table 3. Changes to Table 1 to Evaluate the Effect of Having Pipes Close to the Borehole Wall

	Unit	Semicircle	Quadrant	Double U-Tube
r_{ic}	cm (in.)	4.45 (1.75)		—
t_c		0.4 (0.16)		—
r_{it}		—	—	1.6 (0.63)
t_t		—	—	0.4 (0.16)

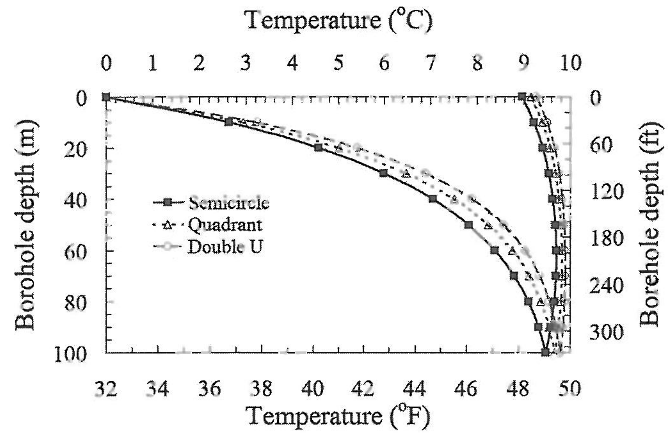

Figure 11 *Fluid temperature profile of semicircle, quadrant and double U-tube configurations with low fluid mass flow rate.*

However, outlet fluid temperatures differ only by 0.26°C (0.47°F).

According to the results for high flow (turbulent regime), it is important to note that the parallel quadrant geometry reverts back to the semicircle geometry. Furthermore, an extra set of walls will result in extra pumping power due to increased wall friction. For cases where the flow is relatively low, the quadrant configuration shows a better performance than the semicircle configuration.

e. Laminar regime

For this last case, the fluid mass flow rate is reduced to 0.03 kg/s (0.066 lb/s) to examine the difference among the various configurations under a laminar regime (i.e., for $Re < 2300$). Even though there is some insulation between channels in the semicircle and quadrant configurations, thermal short circuit has a more pronounced effect on borehole performance compared to high mass flow rate cases. As shown in Figure 11, very small differences are observed between all configurations. For example, the outlet fluid temperature of the double U-tube is only 0.11°C (0.2°F) higher than the quadrant configuration and the borehole thermal resistance of the double U-tube is 2% lower than the quadrant configuration. Contrary to the results presented above, the thermal performance of the quadrant configuration improves marginally over the semicircle configuration since thermal interaction between channels is more significant for low-flow conditions. Furthermore, thermal resistance of the quadrant configuration is 4% lower than for the semicircle configuration.

As shown in Figure 11, the heat is extracted mostly over the first leg. The fluid in the second leg extracts a small amount of heat at the bottom; however, it loses heat while it flows to the top. Therefore, fluid temperature is higher at the bottom of the first leg than at the outlet of the borehole. This is not the desired effect in a borehole and low-flow conditions should be avoided.

Figure 12 presents the difference between the quadrant configuration with perfect insulation (no thermal short circuit) and the double U-tube configuration for the low-flow condition. For the case without thermal interaction between channels, the borehole thermal resistance of the quadrant configuration is lower than that of the double U-tube configuration by 15%. As shown in Figure 12, the fluid temperature increases from 0°C to 9.5°C (32°F to 49.1°F) over the first leg while the increase is about 0.5°C (0.9°F) over the second leg Thus, in a quadrant configuration with perfect insulation, 95% of the heat is extracted in the downward leg while the rest is extracted over the upward leg. Even though the gain in the upward leg is minimal, it is better than for the double U-tube which shows a decrease of the fluid temperature in the upward legs. Consequently, insulated walls between channels are beneficial in the laminar regime.

CONCLUSIONS AND RECOMMENDATIONS

Two nonstandard vertical geothermal borehole configurations are proposed in an attempt to improve the thermal performance of the ground loop portion of ground source heat pump systems. They consist of channels arranged in semicircles and quadrants that are thermally insulated at the common boundaries. These two configurations are proposed to maximize thermal contact with the ground and to minimize thermal interaction between the upward and downward flowing fluid.

The steady-state thermal performance of the proposed configurations is evaluated using an analytical solution for a set of coupled linear differential equations of energy balances for several arrangements with and without thermal interaction. Fluid temperature profiles and borehole thermal resistances are calculated and compared against that of a typical double U-tube configuration.

Results show that in almost all cases studied, the two proposed borehole configurations are superior to the double U-tube configuration. For example, for the reference case (borehole characteristics are listed in Table 1), the borehole thermal resistance of the semicircle is 11% less than that of the double U-tube borehole configuration. Furthermore, a reduction in grout thermal conductivity may cause a larger difference (up to 21%) between the proposed and double U-tube configurations. Large pipe diameters or a close distance between pipes and the borehole wall diminishes the difference between the proposed configurations and the double U-tube configuration. For small fluid flow (laminar regime), insulating the walls between the channels in the proposed configurations is important to reduce the detrimental effect of the thermal short circuit on the borehole thermal performance. It is shown that in the case of a quadrant configuration with perfect insulation, the borehole thermal resistance is 15% less than the one calculated for the double U-tube configuration.

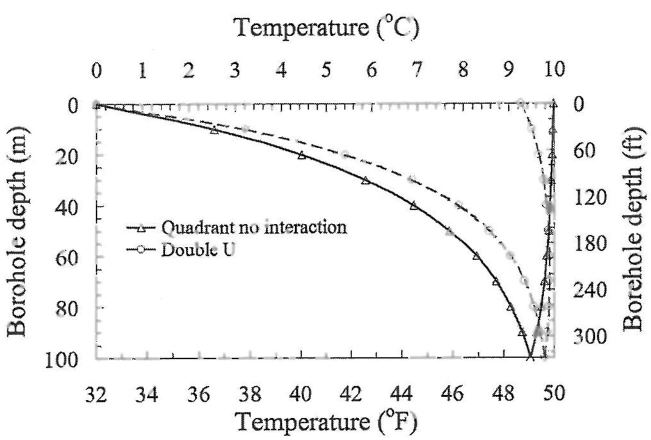

Figure 12 Fluid temperature profile of quadrant configuration with no thermal interaction and double U-tube configuration.

NOMENCLATURE

c_p = heat capacity of the fluid
D_h = hydraulic diameter
h_c = convective heat transfer coefficient of the fluid in the channels
H = borehole depth
k_c = thermal conductivity of the channel wall
k_g = thermal conductivity of the grout
k_{ins} = thermal conductivity of the insulation
k_p = thermal conductivity of the pipe
$\dot{m}$ = mass flow rate in each borehole circuit
$\dot{m}_{total}$ = total mass flow rate of the borehole
Nu = Nusselt number
q' = heat transfer rate to the ground per unit length of the borehole
r_b = borehole radius
r_{ic} internal radius of channels in the semicircle and quadrant
r_{it} = internal radius of pipes in the double U-tube configuration
R^* = dimensionless thermal resistance
R' = thermal resistance per unit length of the borehole

R'_b	=	thermal resistance per unit length
R'_{eff}	=	overall borehole thermal resistance per unit length
Re	=	Reynolds number
t_c	=	wall channel thickness in the semicircle and quadrant configurations
t_{ins}	=	insulation thickness in semicircle and quadrant configurations
t_t	=	pipe thickness in the double U-tube configuration
T_b	=	borehole wall temperature
T_f	=	fluid temperature
T_{in}	=	inlet fluid temperature
z	=	axial coordinate along the borehole depth
Z	=	dimensionless z
θ	=	dimensionless temperature

REFERENCES

Acuna, J., and B. Palm. 2010. Comprehensive summary of borehole heat exchanger research at KTH. Conference on Sustainable Refrigeration and Heat Pump Technology, Stockholm, Sweeden.

Allan, M.L., and S.P. Kavanaugh. 1999. Thermal conductivity of cementitious grouts and impact on heat exchanger length design for ground source heat pumps. *HVAC&R Research* 5(2): 85–96.

Eslami-nejad, P., and M. Bernier. 2011a. Coupling of geothermal heat pumps with thermal solar collectors using double U-tube borehole with two independent circuits. *Applied Thermal Engineering* 31(14–15):3066–77.

Eslami–nejad, P., and M. Bernier. 2011b. Heat transfer in double U-tube boreholes with two independent circuits. *ASME Journal of Heat Transfer* 133(8): 1–12.

Eslami-nejad, P., and M. Bernier. 2012. Freezing of geothermal borehole surroundings: A numerical and experimental assessment with application. *Applied Energy* 98:333–45.

Eslami-nejad, P., and M. Bernier. 2013. A preliminary assessment on the use of phase change materials around geothermal boreholes. *ASHARE Transactions* 119(2)309–11.

Focaccia, S., and F. Tinti 2013. An innovative borehole heat exchanger configuration with improved heat transfer. *Geothermics* 48:93–100.

Gnielinski, V. 1976. New equations for heat and mass transfer in turbulent pipe and channel flow. *International Chemical Engineering* 16(2): 359–68.

Kays, W.M., and M.E. Crawford. 1980. *Convective Heat and Mass Transfer.* New York: McGraw-Hill.

Luo, J., J. Rohn, M. Bayer, and A. Priess. 2013. Thermal performance and economical evaluation of double U-tube borehole heat exchanger with three different borehole diameters. *Energy and Buildings* 67:217–24

Platell, P. 2006. Developing Work on Ground Heat Exchangers. *Proceeding of ECOSTOCK Conference*, 7A-1, Galloway, NJ.

Raymond, J., M. Frenette, A. Léger, E. Magni, and R. Therrien. 2011. Numerical modeling of thermally enhanced pipe performances in vertical ground heat exchangers. *ASHRAE Transactions* 117(1): 1–9.

Remund, C.P. 1999. Borehole thermal resistance: Laboratory and field studies. *ASHRAE Transactions* 105(1): 1–7.

Zeng, H., N. Diao, and Z. Fang. 2003. Heat transfer analysis of boreholes in vertical ground heat exchangers. *International Journal of Heat and Mass Transfer* 46 (23):4467–81.

DISCUSSION

José Acuña, Research Engineer, KTH Royal Institute of Technology, Stockholm, Sweden: Would there be differences in your conclusion for short-term performance? What are the effects of the large temperature differences, i.e., 5 to 7 K? How did you choose the combination flow rate versus depth?

Michel Bernier: This study shows the potential system performance improvement using the two proposed borehole configurations. This work is based on the assumption of a steady-state condition. Therefore, we cannot conclude on the short-term transient performance. Many factors are involved in the evaluation of the short-term performance of such boreholes. For example, the operating period or how often the system is working determine how significant transient effects affect the short-term performance. Perhaps, the next step for us would be to improve the model and evaluate the system operation under real operating conditions.

The temperature difference is not that large, and it is in the range encountered in typical systems. Furthermore, comparing the thermal resistance per unit borehole length of the new configuration against the conventional one can give a good idea of the superior performance of the new configurations.

The selected borehole length and flow rate correspond to typical conditions.

Chuck Gaston, Assistant Professor, Penn State University–York, York, PA: Have you considered unequal cross sections? If the upward path has a smaller cross section, it would have less time for interaction with the downward flow, and the downward flow would have more time for interaction with the earth.

Michel Bernier: Good point. However, we haven't modeled unequal cross sections. It would certainly be worth trying to achieve an optimum design for new configurations.